AIAA JOURNAL
Vol. 39, No. 9, September 2001

Spherical Particle Motion in Harmonic Stokes Flows

C. F. M. Coimbra*
University of Hawaii, Manoa, Honolulu, Hawaii 96822
and
R. H. Rangel†
University of California, Irvine, Irvine, California 92697

An analytical study is presented on the periodic motion of a small particle in a viscous fluid. Previous analytical and numerical contributions to the understanding of particle motion in time-dependent flows are reviewed. Previous works in this field addressed the long-term behavior of the particle (stationary solution) as opposed to the problem treated in this study, which includes initial transient effects. Also presented are the relative scaling of the virtual mass, Stokes, and history drag forces for the long-term solution following the fractional calculus theory. The general solution of the particle momentum equation for unsteady Stokes flows is particularized to a harmonic background fluid velocity. The effect of a nonzero initial relative velocity is studied, and a discussion on the relevance of the results to the Lagrangian simulation of turbulent multiphase flows is presented. The present theoretical results are relevant to the transient motion of small particles in viscous flows such as the ones found in crystal growth processes, fluid markers, and dilute turbulent multiphase flows in general.

Nomenclature

a	=	radius of the particle
$\boldsymbol{a}$	=	dimensionless amplitude of the fluid velocity
$\boldsymbol{b}$	=	dimensionless amplitude of the relative velocity
$\boldsymbol{f}_H$	=	history force
$\boldsymbol{f}_{\mathrm{St}}$	=	Stokes force
$\boldsymbol{f}_{\mathrm{VM}}$	=	virtual mass force
$\boldsymbol{G}$	=	gravitational coefficient, $(1-\alpha)\tau_p \boldsymbol{g}/U_0$
$\boldsymbol{g}$	=	local gravity acceleration
k	=	virtual mass coefficient, $2/(2+\alpha)$
Re_p	=	particle Reynolds number, $a\boldsymbol{W}/\nu$
S	=	scaling number, $\alpha\omega/2 = a^2\Omega/9\nu$
t	=	time
$\hat{t}$	=	dimensionless time, t/τ_p
$\boldsymbol{u}$	=	dimensionless fluid velocity, $\boldsymbol{U}/U_0$
$\boldsymbol{v}$	=	dimensionless particle velocity, $\boldsymbol{V}/U_0$
$\boldsymbol{W}$	=	relative velocity, $\boldsymbol{V}-\boldsymbol{U}$
$\boldsymbol{w}$	=	dimensionless relative velocity, $\boldsymbol{v}-\boldsymbol{u}$
α	=	fluid to particle density ratio, ρ_f/ρ_p
α_c	=	critical density ratio, $\frac{8}{5}$
Δx	=	displacement amplitude of the background flow
η	=	particle to fluid amplitude ratio
η_K	=	Kolmogorov length scale
μ	=	dynamic viscosity
ν	=	kinematic viscosity
ξ	=	$\Delta x/a$
ρ	=	specific mass
τ_K	=	Kolmogorov timescale
τ_p	=	characteristic time, $2\rho_p a^2/9\mu$
ϕ	=	phase difference
Ω	=	angular velocity of the background flow
ω	=	dimensionless angular velocity, $\Omega\tau_p$

I. Motivation

THE purpose of this research is to investigate the unsteady motion of small particles in periodic Stokes flows. Applications of this problem may be found in the settling of particles in colloidal suspensions, in the motion of microbubbles in liquid reservoirs, in the mechanical behavior of fluid markers, and in several other flows of engineering interest, in both laminar and turbulent conditions. The governing equation that describes the motion of rigid particles under these conditions is studied and solved analytically in the present work. This is a classical equation in theoretical fluid mechanics[1] and represents a useful limiting case for problems lying outside of the realm of linear flows.

Crystal growth processes provide some of the most interesting industrial applications that involve the motion of small particles in transient creeping flows. Crystals are grown in a matrix fluid for a variety of applications in the semiconductor and pharmaceutical industries. The possibility of growing near-perfect crystals under microgravity conditions raised the interest of these industries because microgravity crystal growth may well be one of the most promising applications of space technology in the near future. In fact, the most compelling reason to justify orbital flights and the construction of a space station is that some manufacturing technologies that rely on diffusive processes would benefit from low-gravity environments. To be economically viable, the products of such manufacturing industries should concentrate high economic value per mass and per volume besides enjoying a strong benefit from the microgravity environment.

The concept behind microgravity growth of crystals is that, under reduced gravity conditons, the growth of crystals eventually approaches isotropic behavior in the macroscale, provided that the matrix fluid is kept unperturbed. In theory, larger crystals could be eventually grown in a microgravity environment because the crystals do not collapse due to their own weight. The challenge in this case is to seek the most stable conditions for the matrix fluid and to compensate for the inherent corrective motions of a space unit. To meet these challenges it is necessary to study the intricate relationship between the matrix fluid and the particles in suspension.

Both the growth of the crystallizing front and the motion of small, detached structures in the matrix fluid are approximately described by the unsteady diffusion equation in semi-infinite media. In particular, one may retrieve information on slow-motion currents of the matrix fluid through study of the behavior of small marker particles suspended in the matrix. These slow currents caused by the motion of the crystallizing front and by thermal gradients affect the homogeneity of the resulting crystals. To improve the quality of crystals manufactured under microgravity conditions, and to assess the role of low-amplitude disturbances in orbital units, understanding of the unsteady diffusion phenomena involved becomes imperative.

Received 12 May 2000; revision received 16 October 2000; accepted for publication 19 February 2001.

*Assistant Professor, Department of Mechanical Engineering; coimbra@hawaii.edu. Associate Member AIAA.

†Professor, Department of Mechanical and Aerospace Engineering and Department of Chemical and Biochemical Engineering and Material Sciences; rhrangel@uci.edu. Senior Member AIAA.

Recent experimental evidence suggests a much higher occurrence of low-amplitude, high-frequency disturbances (g-jitter) in the Space Shuttle environment than previously expected.[2] These disturbances are inherently periodic and are likely to be a characteristic of any space unit. The unsteady effects of these vibrations on the motion of small particles in the matrix fluid can only be assessed if the equations that describe the creeping flow motion of these particles are understood in detail. The study of these equations, thus, becomes an important step to develop improved crystal-growth technology and may prove to be useful to develop corrective adjustments to reduce the effect of vibrations.

Later in this work, we will show that the motion of a 1-mm-radius spherical crystal of half the density of the matrix fluid is very strongly affected by history effects when experiencing a 60-Hz g-jitter field. The history effects that are originated from the local acceleration term in the Navier–Stokes solution must be included in the formulation of the motion of such crystal particles through the matrix fluid. Inclusion of this important term greatly complicates the analysis of the problem.

II. Background

The first relevant contribution to the study of forces acting on small particles in a viscous fluid is due to Stokes.[3] Stokes derived the well-known expression for the steady-state drag acting on a small sphere that is subjected to a constant freestream flow velocity. The Stokes drag formula relates the force exerted on the sphere to the freestream velocity, the viscosity of the fluid, and the radius of the sphere in a linear way, given that the particle Reynolds number Re_p is maintained much smaller than unity. In fact, the Stokes drag happens to agree well with experiments[4] for values of Reynolds number Re_p up to 1, but this coincidental fact should not be generally extrapolated to unsteady flows. However, recent numerical evidence and a scaling analysis suggest that neglecting the convective contribution results in a small error for oscillating flows at high Strouhal number even for Reynolds number Re_p slightly larger than unity.[5]

Implicit in Stokes' derivation is the premise that the particle is not accelerating with respect to the freestream velocity. In the gravitationally induced motion through a quiescent fluid, the freestream velocity is constant (zero), but the particle accelerates until it reaches its terminal velocity. In this case, and in many others of practical interest, the quasi-steady formulation of the problem incurs an error, and the unsteady contribution from the developing profile near the particle needs to be taken into account.

Boussinesq[6] and Basset[7] independently extended Stokes' derivation to a case where the particle accelerates through the fluid due to a constant gravitational force. Oseen[8] contributed to the previous work of Boussinesq[6] and Basset,[7] concentrating (with little success) on the extension of the previous equations to higher Reynolds number Re_p numbers. The particle equation of motion with a constant forcing (the gravity term) is usually referred to as the BBO equation, due to the original contributions of Boussinesq,[6] Basset,[7] and Oseen.[8] The BBO equation is an integro-differential equation that has a removable singularity in the integrand of the history term. Boggio[9] inverted the BBO equation to derive the velocity history of a small particle moving under the influence of gravity in an otherwise quiescent fluid. This classical result remained the only closed-form solution of the unsteady motion of a small particle in suspension until very recently.

Tchen[1] dealt with the problem of modifying the BBO equation for the case of a uniform but time-dependent freestream flowfield (the freestream flowfield is also called background or unperturbed flowfield in this work). The resulting equation, valid for the limit of infinitesimal particle Reynolds number Re_p and for uniform unsteady background flows, relates the transient acceleration of the particle with the time-dependent freestream or background flow velocity. In this work, this equation is called Tchen's[1] first equation of motion.

In terms of the relative velocity $\boldsymbol{w} = \boldsymbol{v} - \boldsymbol{u}$, where $\boldsymbol{v}$ and $\boldsymbol{u}$ are the particle and the fluid velocity, respectively, Tchen's[1] first equation of motion is written as

$$\frac{\mathrm{d}\boldsymbol{w}}{\mathrm{d}\hat{t}} + k\boldsymbol{w} + \sqrt{\frac{9\alpha}{2}}k\left\{\frac{1}{\sqrt{\pi}}\int_{-\infty}^{\hat{t}}\frac{\mathrm{d}\boldsymbol{w}}{\mathrm{d}\sigma}\frac{\mathrm{d}\sigma}{\sqrt{\hat{t}-\sigma}}\right\} = \boldsymbol{G}k - (1-\alpha)k\frac{\mathrm{d}\boldsymbol{u}}{\mathrm{d}\hat{t}} \tag{1}$$

where velocities are made dimensionless by the flow characteristic velocity U_0. Time is made dimensionless by defining a particle characteristic time τ_p given by $2\rho_p a^2/9\mu$. Here, a is the radius of the spherical particle, ρ_p is the specific mass of the particle, and μ is the dynamic viscosity of the fluid.

The common practice of neglecting the history term in Tchen's[1] first equation has its roots in that, for particles of considerable size, the convective terms become important, and the drag force presents a nonlinear dependence on the relative velocity. This nonlinear dependence can be accurately correlated for the steady-state drag but is unknown for the unsteady term. (For current efforts in modifying the kernel of the history term to include convective effects, see Refs. 5 and 10.) Because there is no analytically derived equation describing the motion of a particle at high particle Reynolds number, there seemed to be little justification for considering the unsteady drag term. In fact, most current calculations use empirical coefficients for the steady-state drag coefficient and neglect completely the evolving profile around the particle, even though the higher Reynolds number Re_p correction for the steady-state drag coefficient is not related to the evolving profile, but only to convective effects.

On the analytical side, two new developments were worth of attention. These were the correct derivation of the momentum equation for small particles in a nonuniform flow, and the calculation of the drag force form for small, nonspherical ellipsoids.[11–14] The analytical attempts to extend the Stokes limit to higher Reynolds numbers met little success,[4,8] and no analytical expression for the momentum equation of particles of any density moving at high particle Reynolds number ($Re_p > 10$) in unsteady flows is known to be accurate. Recently, Kim et al.[5] simulated numerically the convective flow around a heavy solid particle by solving the Navier–Stokes equations and modified the kernel of the history term for the range $1 > Re_p > 100$.

The first relevant work on the derivation of a particle equation of motion valid in non-uniform flows is also due to Tchen,[1] who included an extra term relating the Laplacian of the undisturbed flow velocity to account for the effect of background velocity gradients on the particle acceleration. Many other authors studied Tchen's work and modified the equation proposed by Tchen to account properly for the roles of the pressure gradient and of the flow nonuniformity on the force exerted by the fluid on the particle.[15–18] Maxey and Riley[19] derived a consistent equation of motion for a small particle in nonuniform flows. Some additional modifications of this equation for nonsolid particles have been suggested in recent years.[10,18]

Some conclusions can be drawn from looking back at these previous works concerned with the derivation of a particle momentum equation for unsteady flows. First, the unsteadiness of the evolving flowfield around the particle adds great complexity to the description of the velocity history of the particle, and so it is important to determine exactly when the history effects are important and when they can be neglected. Second, the only term that is significantly affected by the consideration of nonuniform flows is the time derivative of the background flow velocity, which becomes a substantial derivative of the flow velocity at the position of the particle. The substantial derivative makes the equation nonlinear. However, one expects the relationship between the steady-state and the history drag terms not to be greatly affected by this modification, so that conclusions about the relative importance of individual terms in the equation drawn from the study of uniform flows can be extrapolated to nonuniform flows. Third, the attempts to derive an equation valid in nonuniform flows diverted the attention from Tchen's[1] first equation of motion, so that this equation was never solved analytically for a uniform but generic background flow until very recently.[20]

The third conclusion stemming from the preceding paragraph is of great relevance because Tchen's equation[1] has all of the terms of the Maxey–Riley equation,[19] with the exception of the nonlinear substantial derivative and the generally small Faxén corrections. The term represented by the substantial derivative in the Maxey–Riley equation is reduced in Tchen's[1] equation to a time derivative

of the fluid velocity (and valid for uniform or linear background flows).

Before the work of Coimbra and Rangel,[20] the only known analytical solution for the particle velocity including the history drag was the one derived by Boggio.[9] The procedure used by Boggio, and then repeated by Sy et al.,[21] was to solve the equation of motion in Laplace space and then invert back the final solution to time–space. Perhaps because the solution of the integro-differential equation with constant forcing (the gravity acceleration term) was involved, no successful attempts to solve the equation with a time-dependent forcing term were carried out.

Konopliv[22] Laplace-transformed the first-order integro-differential equation of motion for the quiescent-fluid case into a second-order differential equation. Michaelides[23] followed the same procedure, but considered the more involved time-dependent forcing term, instead of the equation with constant forcing considered by Konopliv.[22] Michaelides[23] developed a Laplace-transformation of Tchen's[1] first equation, arriving at a second-order, ordinary differential equation (ODE) for the relative velocity between the particle and the background flow velocity. Michaelides[23] used a standard Runge–Kutta method to solve the equation with unsteady forcing for both the gravitationally induced motion and for a sinusoidally oscillating flow for two oscillating frequencies and two fluid-to-particle density ratios.

Because of the implication to turbulent flows, many authors have focused their attention to particle motion in harmonic Stokes flows. Landau and Lifshitz[24] determined the total drag acting on a small particle that moves harmonically through a quiescent fluid. This problem has important physical implications because it represents one of the simplest particle motions for which the history drag does not asymptote to zero for long times. The derivation presented in the work of Landau and Lifshitz focuses on the drag force for a particle that is moving harmonically in time. The relative velocity between the particle and the far-field flow in this case is exactly described by a sinusoidal function because the background flow is quiescent. Other authors have since analyzed a more realistic case where the background fluid velocity is sinusoidal in time, and the particle is allowed to move under the forces acting on it. This is the problem under study in the present work. Virtual mass effects are included in the analysis as well as the Stokes and history drag forces. We will show that an analytical solution for the velocity of the particle can be found including initial transient effects. Previous works focusing on the harmonic motion of a single particle dealt with the stationary motion,[25–28] which represents the long-term solution only, neglecting the initial transient.

Tchen[1] presented a solution of his first equation of motion for the stationary case and using Fourier analysis (and not the stationary solution) studied the influence of the history term in the motion of the particle. Hinze[25] followed a similar procedure, but represented both velocities of the particle and of the fluid as Fourier integrals. This procedure allows the calculation of approximate amplitude ratios (neglecting an integral phase difference) and phase angles between the particle and the fluid. The procedure used by Hinze is essentially repeated in the work of Hjelmfelt and Mockros,[26] where a more thorough study of the influence of individual terms in the equation of motion is presented. Chao[28] used yet another method to study the equation of motion in the stationary case. In his analysis, Chao Fourier-transformed Tchen's[1] first equation of motion for the stationary case and derived the form of the Lagrangian autocorrelation coefficient. The ratio of particle-to-fluid diffusivity found through Chao's analysis[28] is identical to the one found originally by Tchen.[1] Chao[28] also compared his results with more trivial results found by Soo[16] (who neglected the pressure gradient effect, virtual mass, and history drag forces) and Friedlander[29] (who neglected the virtual mass and history drag forces in his analysis).

Coimbra and Rangel[20] applied a multiple-timescale, fractional-differential linear operator to Eq. (1) transforming it into a second-order ODE and then, using variation of parameters, solved exactly the equation of motion for a small particle in unsteady Stokes flows. The solution presented by Coimbra and Rangel[20] was derived in detail for an initial condition of zero relative velocity between the particle and the fluid. The general solution for an arbitrary initial velocity is shown in the present paper, as a simple extension of the Heaviside problem treated in the original paper.[20] The generalization of the solution for this case is important because it shows that the Laplace transformation of the integro-differential equation for a generic initial condition as performed by Michaelides[23] is not necessary. It suffices to derive the solution of the equation for zero initial velocity and then superimpose the particular solution to the Heaviside problem for a given nonzero initial velocity.

To validate the general solution, three particular flowfields were analyzed in Ref. 20. These three flowfields are the gravitationally induced particle motion, the motion of a particle in a fluid that accelerates linearly in time, and the impulsive start motion of a particle that accelerates in response to a sudden change in velocity of the background fluid velocity. For these flow configurations, the history drag term in the particle equation of motion was asymptotically zero for long times, as opposed to the problem treated in the present work. In the case of harmonic Stokes flows, the history drag term (which is shown below to be proportional to the half-derivative of the relative velocity) is always being regenerated by the continuous contribution of the integer and fractional time derivatives of the relative velocity.

The history term (in curly brackets) in Eq. (1) is identified as the Riemann–Liouville–Weyl half-derivative of the relative velocity $\boldsymbol{w}$ (see Ref. 20). The Riemann–Liouville–Weyl half-derivative of $f(\hat{t})$ is defined as

$$\frac{\mathrm{d}^{\frac{1}{2}} f(\hat{t})}{\mathrm{d}\hat{t}^{\frac{1}{2}}} = \frac{1}{\sqrt{\pi}} \int_{-\infty}^{\hat{t}} \frac{\mathrm{d}f(\sigma)}{\mathrm{d}\sigma} \frac{\mathrm{d}\sigma}{\sqrt{\hat{t}-\sigma}}$$

$$= \frac{1}{\sqrt{\pi}} \int_{0}^{\hat{t}} \frac{\mathrm{d}f(\sigma)}{\mathrm{d}\sigma} \frac{\mathrm{d}\sigma}{\sqrt{\hat{t}-\sigma}} + \frac{f(0)}{\sqrt{\pi \hat{t}}} \tag{2}$$

Thus, Eq. (1) is equivalent to

$$\frac{\mathrm{d}\boldsymbol{w}}{\mathrm{d}\hat{t}} + \sqrt{\frac{9\alpha}{2}} k \frac{\mathrm{d}^{\frac{1}{2}}\boldsymbol{w}}{\mathrm{d}\hat{t}^{\frac{1}{2}}} + k\boldsymbol{w} = \boldsymbol{G}k - (1-\alpha)k\frac{\mathrm{d}\boldsymbol{u}}{\mathrm{d}\hat{t}} \tag{3}$$

To solve Eq. (3) exactly, two conjugate three-timescale linear operators $\Psi^{\pm}$ are defined[20]:

$$\Psi^{\pm} = \frac{\mathrm{d}}{\mathrm{d}\hat{t}} \pm \sqrt{\frac{9\alpha}{2}} k \frac{\mathrm{d}^{\frac{1}{2}}}{\mathrm{d}\hat{t}^{\frac{1}{2}}} + k \tag{4}$$

so that the equation of motion can be rewritten as

$$\Psi^{+}(\boldsymbol{w}) = \boldsymbol{G}k - (1-\alpha)k\frac{\mathrm{d}\boldsymbol{u}}{\mathrm{d}\hat{t}} \tag{5}$$

To make this equation analytically tractable, the conjugate linear operator Ψ^{-} is applied to Eq. (5):

$$\Psi^{-}[\Psi^{+}(\boldsymbol{w})] = \Psi^{-}\left[\boldsymbol{G}k - (1-\alpha)k\frac{\mathrm{d}\boldsymbol{u}}{\mathrm{d}\hat{t}}\right] \tag{6}$$

The linear operation described in Eq. (6) results in a second-order nonhomogeneous linear ODE with constant coefficients.[20] Note that, in transforming Eq. (5) into Eq. (6), no extraneous solution is introduced because the additional initial condition needed to solve the second-order equation is taken directly from the original first-order integro-differential equation.[20] The lower limit of the integral term in Eq. (1) is in fact an initial condition. The second-order equation can be solved exactly by the method of variation of parameters. The mathematical nature of the general solution depends on the sign of the discriminant of the characteristic equation associated with the homogeneous part of the second-order equation. The critical fluid-to-particle density ratio for which the mathematical nature of the solution changes character is $\alpha_c = \frac{8}{5}$. The general solution of the particle equation of motion for values of α larger than α_c is

$$\boldsymbol{w}(\hat{t}) = \left[1 + \sqrt{\frac{9\alpha}{2\Delta}}k^2\left(\frac{e^{R\hat{t}}\mathrm{erfc}(\sqrt{R\hat{t}})}{\sqrt{R}} - \frac{e^{Q\hat{t}}\mathrm{erfc}(\sqrt{Q\hat{t}})}{\sqrt{Q}}\right)\right]\boldsymbol{G}$$
$$+ (1-\alpha)\frac{(e^{Q\hat{t}} - e^{R\hat{t}})}{\sqrt{\Delta}}k\dot{\boldsymbol{u}}(0)$$
$$+ (1-\alpha)\sqrt{\frac{9\alpha}{2\Delta}}k^2\left(\frac{e^{R\hat{t}}\mathrm{erf}(\sqrt{R\hat{t}})}{\sqrt{R}} - \frac{e^{Q\hat{t}}\mathrm{erf}(\sqrt{Q\hat{t}})}{\sqrt{Q}}\right)\dot{\boldsymbol{u}}(0)$$
$$+ \frac{(1-\alpha)ke^{R\hat{t}}}{\sqrt{\Delta}}\int_0^{\hat{t}}\left[e^{-R\tau}\left(\sqrt{\frac{9\alpha}{2\pi}}k\int_0^{\tau}\frac{\ddot{\boldsymbol{u}}(\sigma)\,\mathrm{d}\sigma}{\sqrt{\tau-\sigma}} - \ddot{\boldsymbol{u}} - k\dot{\boldsymbol{u}}\right)\right]\mathrm{d}\tau$$
$$- \frac{(1-\alpha)ke^{Q\hat{t}}}{\sqrt{\Delta}}\int_0^{\hat{t}}\left[e^{-Q\tau}\left(\sqrt{\frac{9\alpha}{2\pi}}k\int_0^{\tau}\frac{\ddot{\boldsymbol{u}}(\sigma)\,\mathrm{d}\sigma}{\sqrt{\tau-\sigma}} - \ddot{\boldsymbol{u}} - k\dot{\boldsymbol{u}}\right)\right]\mathrm{d}\tau \tag{7}$$

whereas for α smaller than α_c, the solution is

$$\boldsymbol{w}(\hat{t}) = \boldsymbol{G} + \frac{2\exp(-b\hat{t}/2)}{\sqrt{|\Delta|}}[\boldsymbol{G} - (1-\alpha)\dot{\boldsymbol{u}}(0)]k\sin\left(\frac{\sqrt{|\Delta|}\hat{t}}{2}\right)$$
$$- \exp(-b\hat{t}/2)\left[\cos\left(\frac{\sqrt{|\Delta|}\hat{t}}{2}\right) + \frac{b}{\sqrt{|\Delta|}}\sin\left(\frac{\sqrt{|\Delta|}\hat{t}}{2}\right)\right]\boldsymbol{G}$$
$$+ \frac{2\exp(-b\hat{t}/2)}{\sqrt{|\Delta|}}\sin\left(\frac{\sqrt{|\Delta|}\hat{t}}{2}\right)\left\{\sqrt{\frac{9\alpha}{2\pi}}k^2[(1-\alpha)\dot{\boldsymbol{u}}(0)\right.$$
$$\left. - \boldsymbol{G}]\int_0^{\hat{t}}\frac{\exp(-b\tau/2)}{\sqrt{\tau}}\cos\left(\frac{\sqrt{|\Delta|}\tau}{2}\right)\mathrm{d}\tau\right.$$
$$+ \int_0^{\hat{t}}\exp(b\tau/2)\cos\left(\frac{\sqrt{|\Delta|}\tau}{2}\right)(1-\alpha)\left(\sqrt{\frac{9\alpha}{2\pi}}k^2\right.$$
$$\left.\times\int_0^{\tau}\frac{\ddot{\boldsymbol{u}}(\sigma)\,\mathrm{d}\sigma}{\sqrt{\tau-\sigma}} - k\ddot{\boldsymbol{u}} - k^2\dot{\boldsymbol{u}}\right)\mathrm{d}\tau\Bigg\}$$
$$- \frac{2\exp(-b\hat{t}/2)}{\sqrt{|\Delta|}}\cos\left(\frac{\sqrt{|\Delta|}\hat{t}}{2}\right)\left\{\sqrt{\frac{9\alpha}{2\pi}}k^2[(1-\alpha)\dot{\boldsymbol{u}}(0) - \boldsymbol{G}]\right.$$
$$\times\int_0^{\hat{t}}\frac{\exp(b\tau/2)}{\sqrt{\tau}}\sin\left(\frac{\sqrt{|\Delta|}\tau}{2}\right)\mathrm{d}\tau$$
$$+ \int_0^{\hat{t}}\exp(b\tau/2)\sin\left(\frac{\sqrt{|\Delta|}\tau}{2}\right)(1-\alpha)$$
$$\left.\times\left(\sqrt{\frac{9\alpha}{2\pi}}k^2\int_0^{\tau}\frac{\ddot{\boldsymbol{u}}(\sigma)\,\mathrm{d}\sigma}{\sqrt{\tau-\sigma}} - k\ddot{\boldsymbol{u}} - k^2\dot{\boldsymbol{u}}\right)\mathrm{d}\tau\right\} \tag{8}$$

In Eqs. (7) and (8), the particle is assumed to be in dynamical equilibrium with the background flow at $\hat{t}=0$, so that $\boldsymbol{w}(0)=0$. Consideration of a generic initial condition is trivial from the solution of the step-function (Heaviside) problem derived by Coimbra and Rangel.[20] The dots denote integer derivatives with respect to $\hat{t}$ or with respect to the dummy variables of integration σ or τ. The following coefficients are used in Eqs. (7) and (8) to simplify the notation: $b=(2k-9\alpha k^2/2)$, $\Delta=b^2-4k^2$, $Q=(-b-\sqrt{\Delta})/2$, and $R=(-b+\sqrt{\Delta})/2$. The general solutions of the equations of motion (7) and (8) are particularized to harmonic Stokes flows in Sec. IV, and the exact solution is compared to the solution found when history effects are neglected.

In Sec. III of this paper, a scaling analysis is performed to derive the frequency range for which the history drag term is important. The scaling analysis shows three different frequency ranges distinguished by the relative importance of the forces in the equation of motion. The low-frequency or Stokes drag range is dominated by the steady-state Stokes drag. At an intermediate frequency, the virtual mass, history, and Stokes drag forces are of the same magnitude. This intermediate frequency range is called in this work critical or viscoelastic frequency range. At higher frequencies, only virtual mass effects are dominant, and thus, this high-frequency range is denominated here virtual mass range. For the scaling analysis presented in Sec. III, the relative velocity is assumed to behave sinusoidally. This assumption is later confirmed by the exact solution of the problem presented in Sec. IV.

III. Relative Scaling of the Virtual Mass, History, and Stokes Drag Forces

Consider the motion of a particle subjected to a freestream flow that behaves sinusoidally in time. After the initial transient caused by the initial condition $\boldsymbol{w}(0)=0$, the particle engages in a motion that can also be very closely approximated by a sinusoidal wave. For scaling purposes, it is considered here that the relative velocity $\boldsymbol{w}$ can also be approximated by a sinusoidal function with the same frequency of the background fluid velocity but with amplitude $\boldsymbol{b}$ and a phase difference. In Sec. IV, the exact analytical solution of the problem is presented, and the scaling analysis performed in the present section is discussed. The virtual mass, history, and Stokes drag forces are thus given by

$$\boldsymbol{f}_{\mathrm{VM}} = \frac{\alpha}{2}\frac{\mathrm{d}\boldsymbol{w}}{\mathrm{d}\hat{t}} \cong \frac{\boldsymbol{b}\alpha}{2}\frac{\mathrm{d}[\sin(\omega\hat{t})]}{\mathrm{d}\hat{t}} = \frac{\boldsymbol{b}\alpha\omega\cos(\omega\hat{t})}{2} \cong \mathcal{O}\left(\boldsymbol{b}\frac{\alpha\omega}{2}\right) \tag{9}$$

$$\boldsymbol{f}_H = \sqrt{\frac{9\alpha}{2}}\frac{\mathrm{d}^{\frac{1}{2}}\boldsymbol{w}}{\mathrm{d}\hat{t}^{\frac{1}{2}}} \cong \boldsymbol{b}\sqrt{\frac{9\alpha\omega}{2}}\frac{\mathrm{d}^{\frac{1}{2}}[\sin(\omega\hat{t})]}{[\mathrm{d}(\omega\hat{t})]^{\frac{1}{2}}}$$
$$\cong \boldsymbol{b}\sqrt{\frac{9\alpha\omega}{2}}\sin(\omega\hat{t}+\pi/4) \cong \mathcal{O}\left(\boldsymbol{b}\sqrt{\frac{9\alpha\omega}{2}}\right) \tag{10}$$

$$\boldsymbol{f}_{\mathrm{St}} = \boldsymbol{w} \cong \boldsymbol{b}\sin(\omega\hat{t}) \cong \mathcal{O}(\boldsymbol{b}) \tag{11}$$

Note that for the history drag force, the generalized chain rule for fractional derivatives is used. The chain rule for a generic differintegral operation is given by[30]

$$\frac{\mathrm{d}^n f[g(x)]}{\mathrm{d}x^n} = \frac{f[g(x)]}{x^n\Gamma(1-n)} + \sum_{j=1}^{\infty}\binom{n}{j}\frac{x^{j-n}}{\Gamma(j-n+1)}j!$$
$$\times\sum_{m=1}^{j}f^m\sum\prod_{k=1}^{j}\frac{1}{P_k!}\left[\frac{f^k}{k!}\right]^{P_k} \tag{12}$$

where the last summation extends over all combination of nonnegative integer values of P_k such that

$$\sum_{k=1}^{n}kP_k = n \tag{13}$$

$$\sum_{k=1}^{n}P_k = m \tag{14}$$

For $g(x)=\omega x$, the generalized chain rule gives simply

$$\frac{\mathrm{d}^n f(\omega x)}{\mathrm{d}x^n} = \omega^n\frac{\mathrm{d}^n f(\omega x)}{[\mathrm{d}(\omega x)]^n} \tag{15}$$

The relative scaling of the three dimensionless forces is, thus,

$$\langle|\boldsymbol{f}_{\mathrm{VM}}| : |\boldsymbol{f}_H| : |\boldsymbol{f}_{\mathrm{St}}|\rangle = \left\langle S : 3S^{\frac{1}{2}} : 1\right\rangle \tag{16}$$

where $S=\alpha\omega/2$. The maximum influence of the history drag occurs when $\partial\{|\boldsymbol{f}_H|/(|\boldsymbol{f}_{\mathrm{VM}}+\boldsymbol{f}_H+\boldsymbol{f}_{\mathrm{St}}|)\}/\partial S=0$, which corresponds to $S=1$ or $\alpha\omega=2$. Note that, taking into account the different phases of the three forces, the amplitude of the total force is $|\boldsymbol{f}_{\mathrm{VM}}+\boldsymbol{f}_H+\boldsymbol{f}_{\mathrm{St}}| = (S^2+3\sqrt{2}S^{3/2}+9S+3\sqrt{2}S^{1/2}+1)^{1/2}$. The scaling relation (16) shows that when $S\sim 1$ the amplitude of the history drag force is approximately three times larger than the amplitude of the virtual mass and the Stokes drag forces. When the value of S is much smaller than 1, the Stokes drag dominates. For

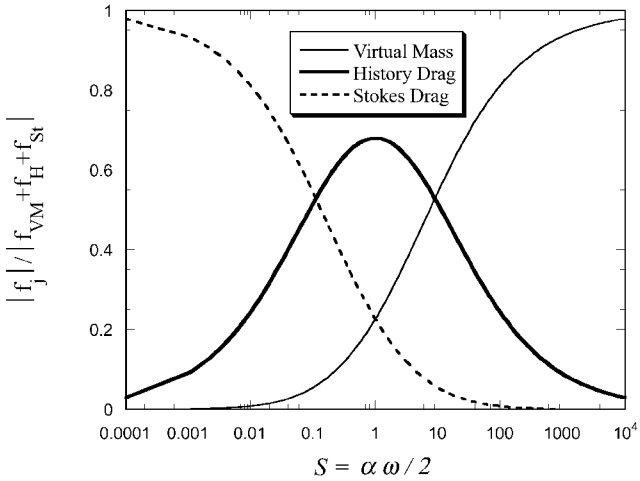

Fig. 1 Relative scaling of the virtual mass, history, and Stokes drag forces.

values of S much larger than 1, the virtual mass force (caused by pressure gradients) is dominant. Figure 1 shows graphically the contribution of the three individual forces as a function of the scaling number S.

Note that the scaling number S does not depend on the density of the particle. The dimensionless number that governs the scaling of the forces is

$$S = \alpha\omega/2 = (\Omega/\nu)(a/3)^2 \tag{17}$$

where Ω is the dimensional forcing frequency.

Note that the present scaling analysis gives only a limited view of the actual behavior of the particles. This is because only the relative scaling of the forces that depend on the velocity driving potential is determined by the analysis. The actual velocity response of the particle can only be determined from the solution of the equation of motion including the initial transients.

IV. Stationary Analysis

The stationary regime, that is, the solution of Eq. (1) neglecting the initial transients, has been studied by several authors in the past.[1,25–28] Although the specifics of the techniques used by the previous authors vary, the basic idea is the same: The velocity of the background fluid and the velocity of the particle are expressed as sinusoidal functions. In particular, these velocities can be expressed as Fourier integrals of the form[25,26]

$$u_i = \int_0^\infty (\zeta \cos\omega\hat{t} + \lambda \sin\omega\hat{t})\, d\omega \tag{18}$$

$$v_i = \int_0^\infty (\chi \cos\omega\hat{t} + \varphi \sin\omega\hat{t})\, d\omega \tag{19}$$

The velocities given by Eqs. (18) and (19) are then forced to satisfy Eq. (1), and the velocity of the particle is then expressed as

$$v_i = \int_0^\infty \eta[\zeta \cos(\omega\hat{t} + \phi) + \lambda \sin(\omega\hat{t} + \phi)]\, d\omega \tag{20}$$

where

$$\eta = \sqrt{(1 + g_1)^2 + g_2^2} \tag{21}$$

$$\phi = \tan^{-1}[g_2/(1 + g_1)] \tag{22}$$

The two auxiliary functions $g_1(S, \alpha)$ and $g_2(S, \alpha)$ are calculated from the algebraic substitution of Eqs. (18) and (19) into Eq. (1) (Ref. 25). The main results of the stationary analysis are shown in Fig. 2, which shows the particle-to-fluid amplitude ratio η and the phase difference ϕ as a function of the scaling number S.

In crystal growth processes, the value of α is typically close to unity. Figure 3 shows that the maximum phase difference for the case of $\alpha = 2$ is 5.85 deg, which occurs for $S = 1.41$ (conditions

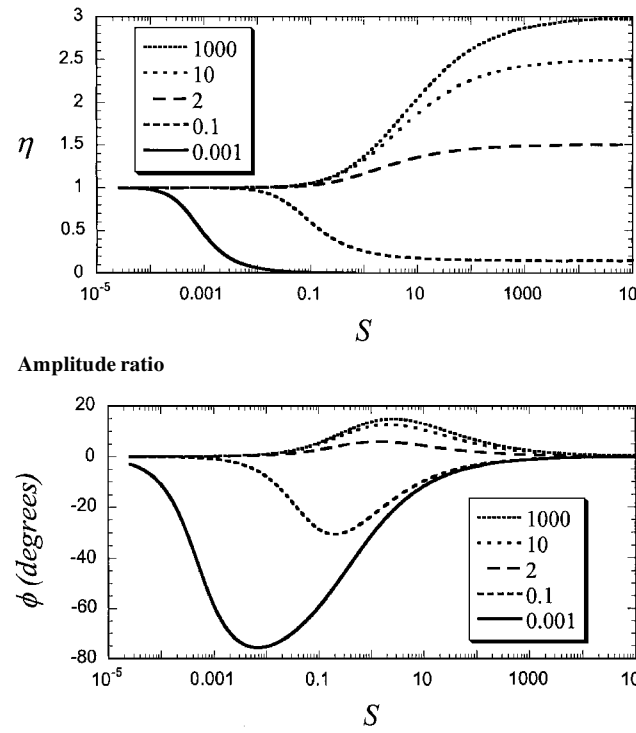

Fig. 2 Different values of α.

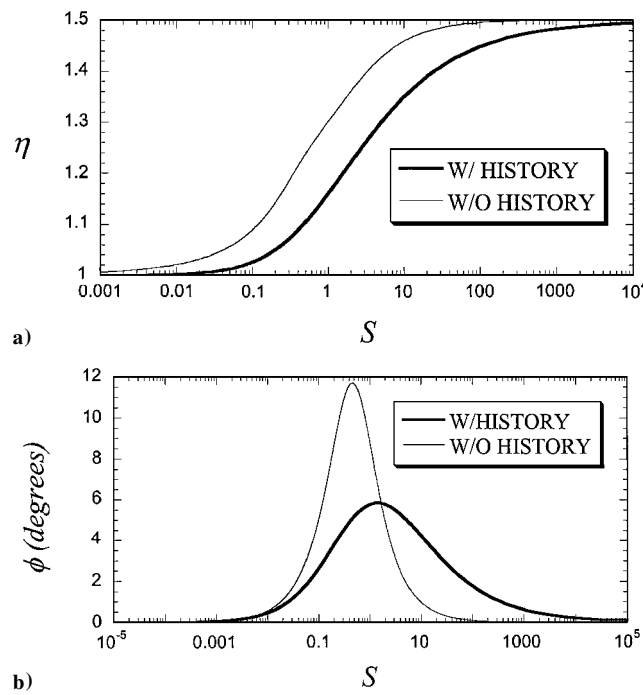

Fig. 3 Amplitude ratio and phase difference for $\alpha = 2$.

found for, e.g., $f \sim 85$ Hz in a 40 cS solution and for a particle radius $a = 1$ mm). For $S = 1$ ($f \sim 60$ Hz, same conditions as earlier), the phase advance of the light particle in question is 5.78 deg. The amplitude ratio for $S = 1$ is equal to 1.16 when history effects are considered. The amplitude ratio is equal to 1.30 when history effects are neglected. The small values for the phase difference in this particular case make the simplified scaling analysis for the ratio of the forces very accurate (see Figs. 2 and 3). Note that the preceding negative phase differences indicate phase delay (heavy particles). Conversely, positive phase differences indicate phase advance (light particles).

It can also be inferred from Fig. 2 that, for the case $\alpha = 2$ and for $S > 1000$, the phase difference is negligible and the amplitude

ratio approaches the asymptotic value of 1.50. Figure 3 shows the comparison between the long-term solution that includes the history contribution and the one that neglects it, for the amplitude and phase difference and for the case $\alpha = 2$. Note the significant difference in phase advance obtained when history effects are taken into account. We will address the case $\alpha = 2$ in more detail with the full solution of the equation of motion in the next section.

V. Solution of the Equation of Motion for Harmonic Stokes Flows

The general solutions (7) and (8) are particularized to a background fluid velocity $\boldsymbol{u} = \boldsymbol{a}\sin(\omega\hat{t})$, yielding for $\alpha > \frac{8}{5}$,

$$\begin{aligned}\boldsymbol{w}(\hat{t}) = {} & \frac{\boldsymbol{a}(1-\alpha)k\omega e^{Q\hat{t}}}{\sqrt{\Delta}}\left[1-\left(\frac{\omega^2-Qk}{Q^2-\omega^2}\right)-\sqrt{\frac{9\alpha}{2Q}}k\,\mathrm{erf}(\sqrt{Q\hat{t}})\right] \\ & -\frac{\boldsymbol{a}(1-\alpha)k\omega e^{R\hat{t}}}{\sqrt{\Delta}}\left[1-\left(\frac{\omega^2-Rk}{R^2-\omega^2}\right)-\sqrt{\frac{9\alpha}{2R}}k\,\mathrm{erf}(\sqrt{R\hat{t}})\right] \\ & +\frac{\boldsymbol{a}(1-\alpha)k\omega}{\sqrt{\Delta}}\left[\frac{(k+Q)\omega}{Q^2+\omega^2}-\frac{(k+R)\omega}{R^2+\omega^2}\right]\sin(\omega\hat{t}) \\ & +\frac{\boldsymbol{a}(1-\alpha)k\omega}{\sqrt{\Delta}}\left[\frac{Rk-\omega^2}{R^2+\omega^2}-\frac{Qk-\omega^2}{Q^2+\omega^2}\right]\cos(\omega\hat{t}) \\ & +\frac{\boldsymbol{a}(1-\alpha)k^2\omega^2}{\sqrt{\Delta}}\sqrt{\frac{9\alpha}{2R}} \\ & \times\begin{Bmatrix} e^{Q\hat{t}}\displaystyle\int_0^{\hat{t}}\left[e^{-Q\tau}\left(\int_0^{\tau}\frac{\sin(\omega\sigma)\,\mathrm{d}\sigma}{\sqrt{\tau-\sigma}}\right)\right]\mathrm{d}\tau \\ -e^{R\hat{t}}\displaystyle\int_0^{\hat{t}}\left[e^{-R\tau}\left(\int_0^{\tau}\frac{\sin(\omega\sigma)\,\mathrm{d}\sigma}{\sqrt{\tau-\sigma}}\right)\right]\mathrm{d}\tau \end{Bmatrix} \\ & +\frac{\boldsymbol{w}(0^+)}{\sqrt{Q}-\sqrt{R}}\begin{bmatrix} e^{R\hat{t}}\sqrt{R}\,\mathrm{erfc}(\sqrt{R\hat{t}}) \\ -e^{Q\hat{t}}\sqrt{Q}\,\mathrm{erfc}(\sqrt{Q\hat{t}})\end{bmatrix}\end{aligned} \tag{23}$$

and for $\alpha < \frac{8}{5}$,

$$\begin{aligned}\boldsymbol{w}(\hat{t}) = {} & \frac{2\boldsymbol{a}\omega(1-\alpha)\exp(-b\hat{t}/2)}{\sqrt{|\Delta|}}\sqrt{\frac{9\alpha}{2\pi}}k^2\begin{Bmatrix}\sin\left(\frac{\sqrt{|\Delta|}\hat{t}}{2}\right)\displaystyle\int_0^{\hat{t}}\frac{\exp(b\tau/2)}{\sqrt{\tau}}\cos\left(\frac{\sqrt{|\Delta|}\tau}{2}\right)\mathrm{d}\tau \\ -\cos\left(\frac{\sqrt{|\Delta|}\hat{t}}{2}\right)\displaystyle\int_0^{\hat{t}}\frac{\exp(b\tau/2)}{\sqrt{\tau}}\sin\left(\frac{\sqrt{|\Delta|}\tau}{2}\right)\mathrm{d}\tau\end{Bmatrix} \\ & +\frac{2\boldsymbol{a}\omega^2(1-\alpha)\exp(-b\hat{t}/2)}{\sqrt{|\Delta|}}\sqrt{\frac{9\alpha}{2\pi}}k^2\begin{Bmatrix}\cos\left(\frac{\sqrt{|\Delta|}\hat{t}}{2}\right)\displaystyle\int_0^{\hat{t}}\left[\exp(b\tau/2)\sin\left(\frac{\sqrt{|\Delta|}\tau}{2}\right)\int_0^{\tau}\frac{\sin(\omega\sigma)}{\sqrt{\tau-\sigma}}\mathrm{d}\sigma\right]\mathrm{d}\tau \\ -\sin\left(\frac{\sqrt{|\Delta|}\hat{t}}{2}\right)\displaystyle\int_0^{\hat{t}}\left[\exp(b\tau/2)\cos\left(\frac{\sqrt{|\Delta|}\tau}{2}\right)\int_0^{\tau}\frac{\sin(\omega\sigma)}{\sqrt{\tau-\sigma}}\mathrm{d}\sigma\right]\mathrm{d}\tau\end{Bmatrix} \\ & +\frac{2\boldsymbol{a}\omega(1-\alpha)\exp(-b\hat{t}/2)}{\sqrt{|\Delta|}}\begin{Bmatrix}\sin\left(\frac{\sqrt{|\Delta|}\hat{t}}{2}\right)\displaystyle\int_0^{\hat{t}}\exp(b\tau/2)\cos\left(\frac{\sqrt{|\Delta|}\tau}{2}\right)[\omega\sin(\omega\tau)-k\cos(\omega\tau)]\,\mathrm{d}\tau \\ -\cos\left(\frac{\sqrt{|\Delta|}\hat{t}}{2}\right)\displaystyle\int_0^{\hat{t}}\exp(b\tau/2)\sin\left(\frac{\sqrt{|\Delta|}\tau}{2}\right)[\omega\sin(\omega\tau)-k\cos(\omega\tau)]\,\mathrm{d}\tau\end{Bmatrix} \\ & +\boldsymbol{w}(0^+)\sqrt{\frac{9\alpha}{8\pi}}ke^{-b\hat{t}/2}\left\{\left[\sqrt{|\Delta|}\sin\left(\frac{\sqrt{|\Delta|}\hat{t}}{2}\right)+b\cos\left(\frac{\sqrt{|\Delta|}\hat{t}}{2}\right)\right]\int_0^{\hat{t}}\frac{\exp(b\tau/2)}{\sqrt{\tau}}\sin\left(\frac{\sqrt{|\Delta|}\tau}{2}\right)\mathrm{d}\tau\right. \\ & \left.-\left[b\sin\left(\frac{\sqrt{|\Delta|}\hat{t}}{2}\right)-\sqrt{|\Delta|}\cos\left(\frac{\sqrt{|\Delta|}\hat{t}}{2}\right)\right]\int_0^{\hat{t}}\frac{\exp(b\tau/2)}{\sqrt{\tau}}\cos\left(\frac{\sqrt{|\Delta|}\tau}{2}\right)\mathrm{d}\tau\right\} \\ & +\boldsymbol{w}(0^+)\left[\frac{(2k-b)\exp(-b\hat{t}/2)}{\sqrt{|\Delta|}}\sin\left(\frac{\sqrt{|\Delta|}\hat{t}}{2}\right)-\exp(-b\hat{t}/2)\cos\left(\frac{\sqrt{|\Delta|}\hat{t}}{2}\right)\right]\end{aligned} \tag{24}$$

The terms multiplying $\boldsymbol{w}(0^+)$ in both Eqs. (23) and (24) relate to a nonzero initial velocity.[20] If the history term contribution is neglected, the solution of the simplified equation of motion is given simply by (where subscript for no history is nh) is

$$\boldsymbol{w}_{\mathrm{nh}}(\hat{t}) = (1-e^{-k\hat{t}})\boldsymbol{G}-Pke^{-k\hat{t}}\int_0^{\hat{t}}e^{k\sigma}\dot{\boldsymbol{u}}(\sigma)\,\mathrm{d}\sigma+\boldsymbol{w}_{\mathrm{nh}}(0^+)e^{-k\hat{t}} \tag{25}$$

which gives for a sinusoidal background velocity

$$\begin{aligned}\boldsymbol{w}_{\mathrm{nh}}(\hat{t}) = {} & \frac{\boldsymbol{a}\omega k(1-\alpha)}{k^2+\omega^2}[ke^{-k\hat{t}}-k\cos(\omega\hat{t})-\omega\sin(\omega\hat{t})] \\ & +\boldsymbol{w}_{\mathrm{nh}}(0^+)e^{-k\hat{t}}\end{aligned} \tag{26}$$

Figure 4 shows the particle velocity behavior given by solutions (23–25) for different values of the fluid-to-particle density ratio and dimensionless forcing frequencies for $\boldsymbol{w}(0^+) = 0$. The range of values of the product $\alpha\omega$ covered in these Figs. 4 is $[10^{-3} : 10^5]$, varying from the steady-state Stokes drag regime to the virtual mass force regime. The thick lines in Figs. 4a–4c indicate the full solutions (23) and (24). The thin lines indicate the behavior given by the no-history solution (26). Figure 4 show the increasing influence of the history term when the scaling number S approaches the value of 1 from both sides of the spectrum of frequencies. Of particular interest is that the absolute maximum of the relative velocity $\boldsymbol{w}$ is always smaller than the absolute maximum of its no-history counterpart $\boldsymbol{w}_{\mathrm{nh}}$, although it is of the same order of magnitude. After the initial exponential decay, the amplitude of the relative velocity $\boldsymbol{w}_{\mathrm{nh}}$ is of order $\omega|\alpha-1|k(k+\omega)/(k^2+\omega^2)$.

Another interesting feature shown in Fig. 4 is the phase difference between the fluid velocity and the particle velocity. For particles heavier than the fluid, there is a phase lag caused by the inability of the particle to respond rapidly to fluid velocity variations due to its larger inertia. For the case of the light particles, the situation is reversed because of the combined effect of the history drag and virtual mass forces. The phase difference for light particles is positive because the relative acceleration is very important to determine the particle behavior. This becomes clear when it is observed that, for a light particle, the particle velocity always changes sign before the fluid velocity does it. If the force on the particle were only a function of the relative velocity (as in the quasi-steady formulation), this

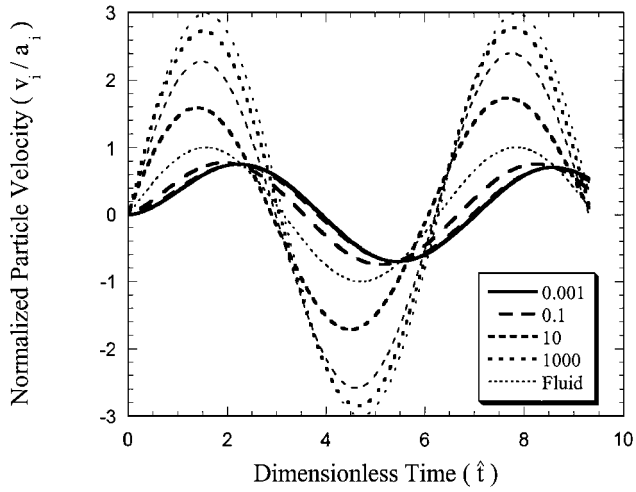

a) $\omega = 1$

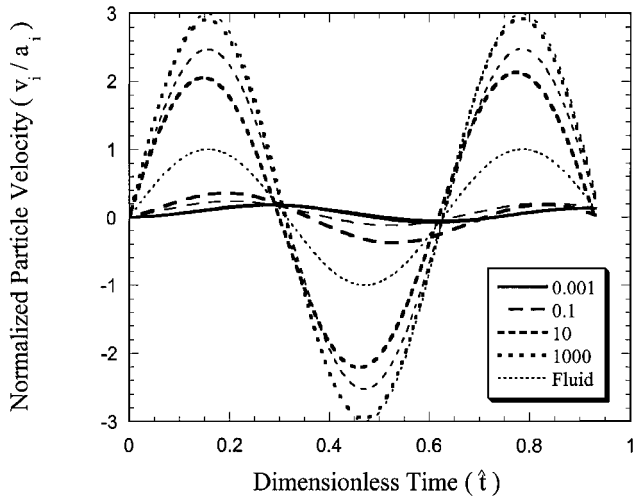

b) $\omega = 10$

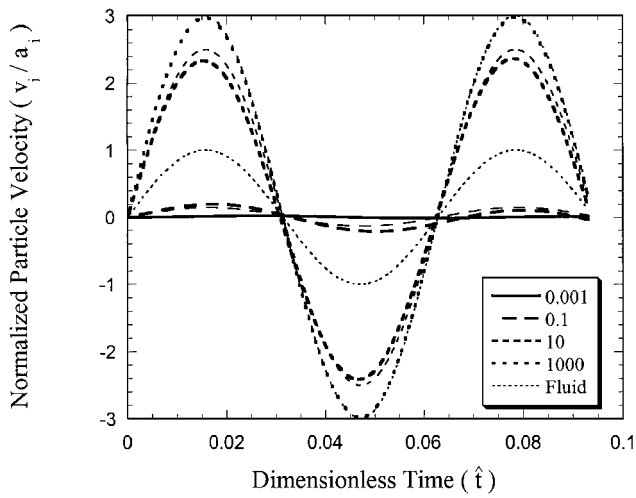

c) $\omega = 100$

Fig. 4 Normalized particle velocities for different values of α; thick lines represent the full solutions (23) and (24) and the thin lines the solution neglecting history effects (26).

behavior would not be predicted. The actual behavior of light particles shows how much the pressure and stress gradients due to the time derivatives of the relative velocity affect the forces on a particle with smaller inertia.

That light particles are heavily influenced by the time derivatives of the relative velocity is clearly understood if one thinks of a suspended bubble in a fluid moving with constant velocity. If the fluid is moving for a time much longer than the response time of the bubble (which due to virtual mass effects is better characterized as τ_p/k), the particle will move with zero relative velocity with respect to the fluid. To a fixed observer, the bubble is moving with the fluid velocity. Now, if the fluid acquires a constant negative acceleration, the bubble also starts accelerating in the negative direction. After a sufficient time, the bubble reaches its terminal velocity associated with the deceleration rate of the fluid. For the fixed observer, the bubble will be moving with the decreasing velocity of the fluid plus its terminal velocity. When the velocity of the fluid reaches a value equal to minus the terminal velocity of the bubble, the bubble is at rest for the fixed observer. The time for the fluid to reach zero velocity from that point on is a phase lag for the fluid: The bubble is already moving with respect to the fixed observer, but the fluid has not reached zero velocity yet. This simple example of linear acceleration shows the importance of the combined virtual mass and acceleration drag forces. The term acceleration drag was used to describe the history drag[1] but it is not very adequate because of the half-derivative dependence on the relative velocity that the history term presents, and not on the first derivative. The terminology is, however, interesting for emphasizing the dependence of bubble behavior on the acceleration of the fluid (or perhaps, on the half-acceleration, too).

The phase diagrams shown in Fig. 5 show the initial transient behavior of the particles before they attain an orbital trajectory. As in Fig. 4, the thick lines represent the full solutions and the thin lines the no-history solution. Because of their larger inertia, the phase trajectories of particles with density larger than the fluid converge inward from the circle that represents the trajectory of a fluid particle. The light particles are confined to the region limited by the fluid particle circle in the interior, by the $[-3:3]$ range on the velocity axis, and by the $[-1/\omega : 6\omega]$ on the displacement axis. Figure 5a shows the very different trajectory described by the full solution and the quasi-steady solution for $\alpha = 10$. The difference in trajectories for this particular value of α decreases as the forcing frequency increases from Figs. 5a to 5c because this light particle enters the virtual mass regime $S \gg 10$. The phase diagrams have the advantage of accentuating the differences between the curves for the full solution and for the quasi-steady solutions when compared to the usual velocity vs time representation. Note that all curves agree with the scaling analysis of Sec. III in the sense that history effects are important when the product S approaches the critical value of 1 and become less important when departing from this value for both sides of the spectrum of S.

The constraint of small particle Reynolds number Re_p places a tight limit on the displacement amplitude for which it is possible to reach the critical or viscoelastic regime ($S \sim 1$), where history effects are dominant [see Eq. (17)]. The particle Reynolds number Re_p is given by

$$Re_p(\hat{t}) \equiv a|\boldsymbol{V} - \boldsymbol{U}|/\nu = aU_0|\boldsymbol{w}(\hat{t})|/\nu = 9S\xi|\boldsymbol{w}(\hat{t})| \qquad (27)$$

Equation (27) restricts the dimensionless displacement amplitude of the background flow $\xi = \Delta x/a$ to satisfy the condition

$$\xi \ll 1/9S|\boldsymbol{w}(\hat{t})| \qquad (28)$$

Equation (28) shows that to approach the viscoelastic regime ($S \sim 1$) in Stokes flow for background fluid displacements larger than the particle radius, the density of the particle has to be very similar to the density of the fluid. If the fluid-to-particle density ratio deviates even slightly from 1, the fluid displacement has to be only a fraction of the particle radius. Thus, to comply with the restriction on Reynolds number Re_p for particles with density differing from the density of the fluid and to have significant history effects, the displacement amplitude of the background flow has to be of the order of the radius of the particle, or smaller. If the amplitude of the oscillations increase, the small Reynolds number Re_p restriction is not satisfied, and the convective terms in the Navier–Stokes equation cannot be neglected. Because higher-order approximations on Reynolds number Re_p predict lesser effects of the history term contribution with increasing Reynolds number Re_p (Ref. 31), Eq. (28) gives an upper bound for the amplitude of displacement oscillations that are strongly affected by the history drag. In other words, history drag effects in harmonic flows are maximized when the forcing

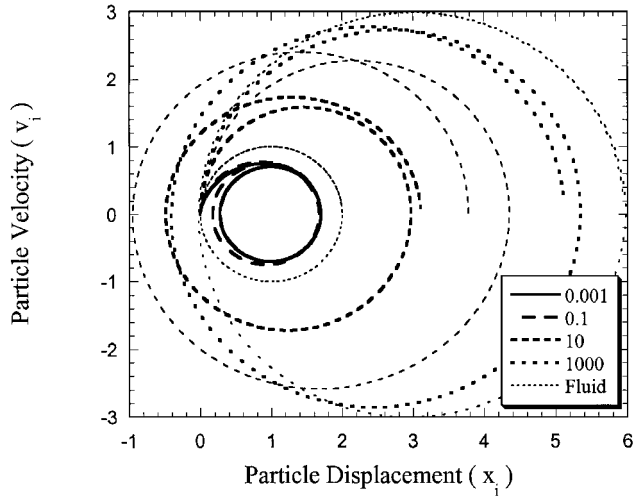

a) $\omega = 1$

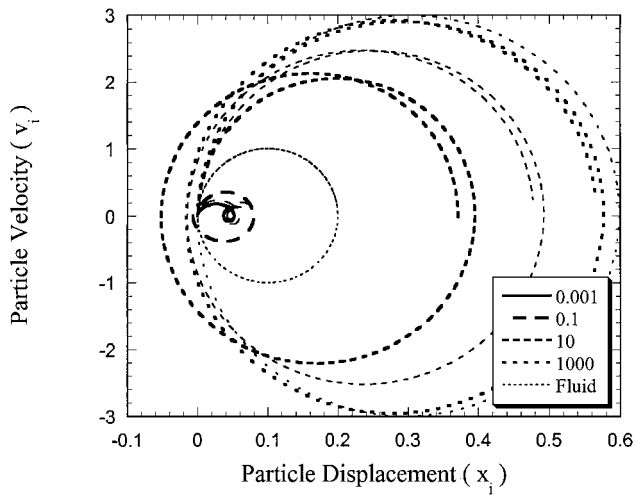

b) $\omega = 10$

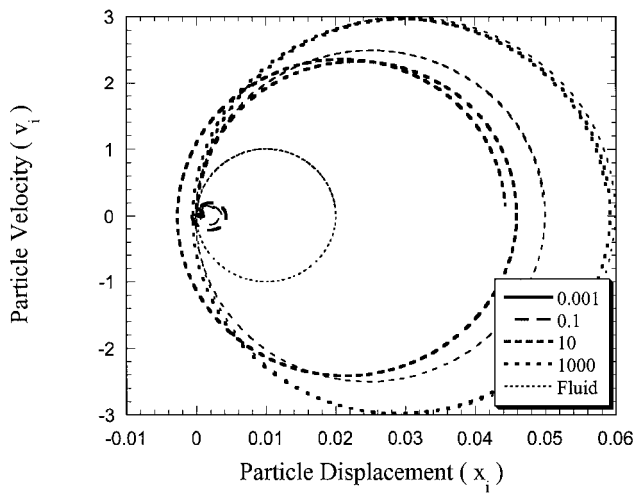

c) $\omega = 100$

Fig. 5 Phase diagrams for different values of α; thick lines represent the full solutions (23) and (24) and the thin lines the solution neglecting the history term (26).

frequency approaches the value $\Omega \sim 9\nu/a^2$ and for displacement amplitudes smaller than the radius of the particle.

The behavior of Reynolds number Re_p is shown in Fig. 6 for a background fluid velocity $\boldsymbol{u} = \boldsymbol{a}\sin(\omega \hat{t})$ and for the case $\alpha = 2$ and $S = 1$. It can be inferred from Fig. 6 that for zero injection velocity, the stationary behavior is attained during the first half-period (one crest). For the case of zero initial relative velocity, the consideration of history effects leads always to a smaller value of Reynolds number Re_p when compared to the no-history analysis. Note also that the fluid displacement has to be of the order of $\frac{1}{10}$ of the particle radius a to comply with the restriction $Re_p < 1$. Figure 7 shows the behavior of Reynolds number Re_p for different (positive) injection velocities. For $\boldsymbol{v} = +1$, the stationary behavior is obtained only after a full period (two crests). This case corresponds to an injection velocity of the same magnitude of the velocity amplitude of the background flow. For $\boldsymbol{v} = +10$, the stationary behavior is not attained even after three full periods. Note the sharp difference in initial decay rate when history effects are considered. For $\boldsymbol{v} = +100$, the oscillations of the first two periods are almost completely suppressed when history effects are considered but are evident when history effects are neglected. When history effects are neglected, the particle starts oscillating after $\hat{t} \sim 9.5$, much earlier than the time predicted when history effects are considered ($\hat{t} \sim 16.5$). Figure 8 shows equivalent plots for negative injection velocities $\boldsymbol{v} = -1$, -10, and -100. Figure 8 shows a slightly different behavior due to the phase difference caused by the negative velocities. Note that when the amplitude of $|\boldsymbol{v}|$ is much larger ($|\boldsymbol{v}| \sim 100$) than the amplitude of the background flow ($|\boldsymbol{a}| = 1$), the maximum value of Reynolds number Re_p is

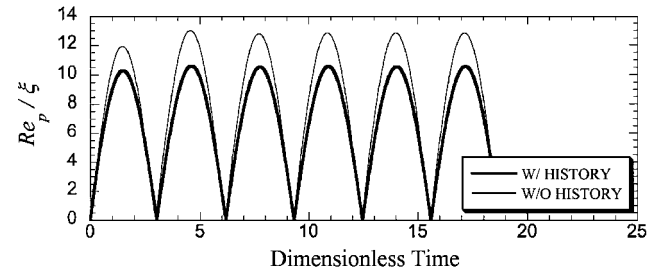

Fig. 6 Reynolds number Re_p behavior for $S = 1$, $\alpha = 2$, and zero initial velocity $v(0) = 0$.

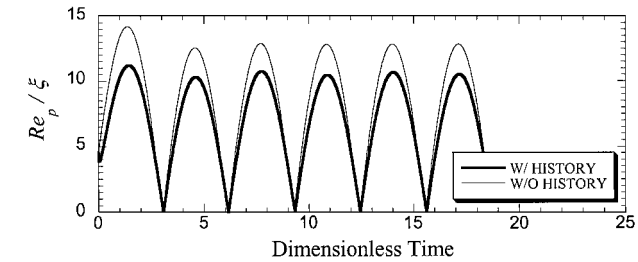

$v(0) = -1$

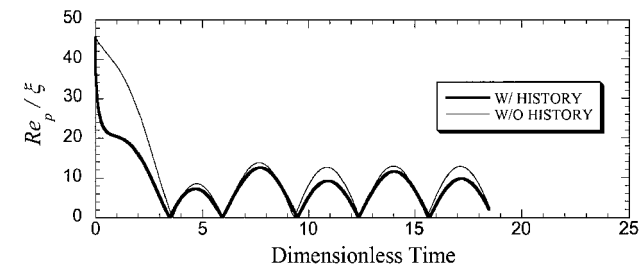

$v(0) = -10$

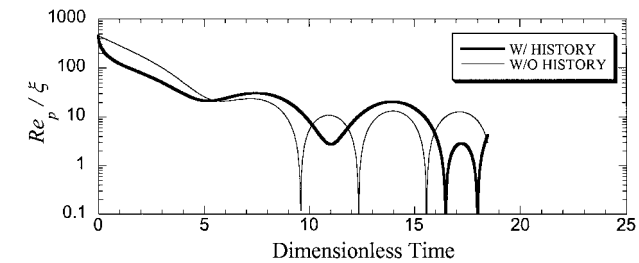

$v(0) = -100$

Fig. 7 Reynolds number Re_p behavior for $S = 1$, $\alpha = 2$, and nonzero initial velocities.

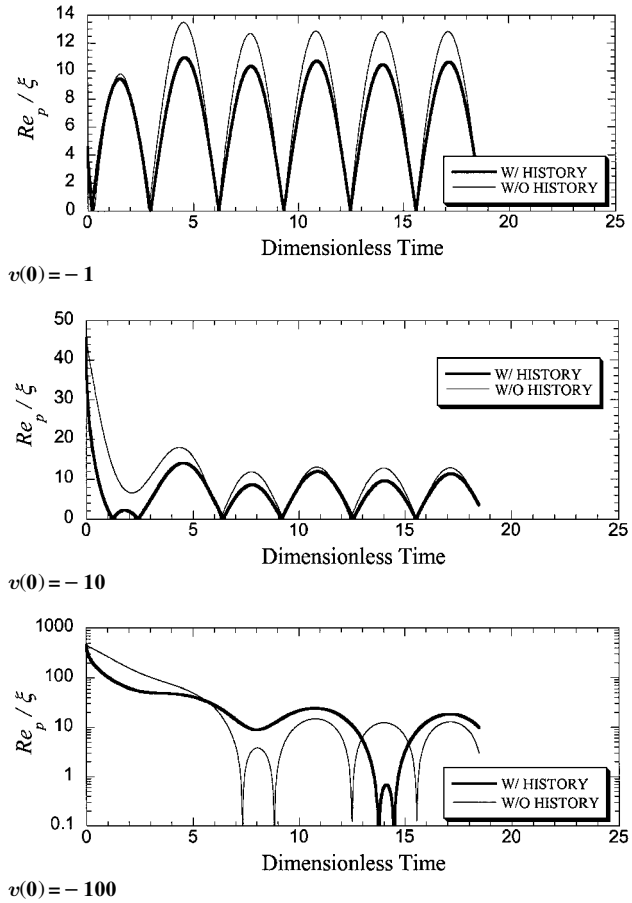

Fig. 8 Reynolds number Re_p behavior for $S = 1$, $\alpha = 2$, and nonzero initial velocities.

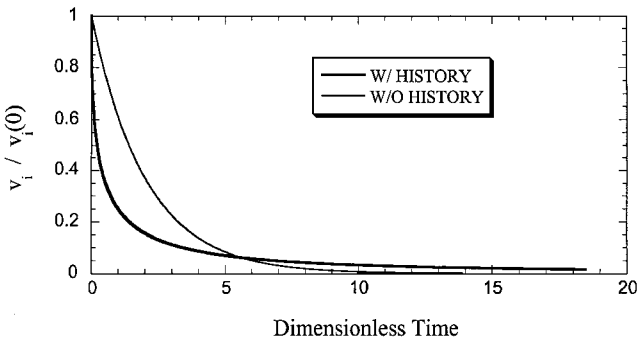

Fig. 9 Initial decay for nonzero initial velocities; $\alpha = 2$.

underpredicted when history effects are neglected. This underprediction is because the decay of the initial velocity effect is underpredicted for short times and overpredicted for long times when history effects are neglected. This becomes clear when the decay of a generic initial particle velocity is plotted as in Fig. 9. For $|v| \sim 100$, the oscillations of the background flow only become important for long times ($\hat{t} > 5.5$), which correspond to the range where the relative velocity is underpredicted when history effects are neglected.

VI. Implications to Lagrangian Simulations of Turbulent Multiphase Flows

As a simplified model, and in a modal sense, the smaller scales of the frequency spectrum of turbulence can be approximated by superposition of harmonic oscillations. The restriction on displacement amplitude found in the preceding analysis is, thus, relevant to assess the effects of virtual mass and history forces in particle dispersion studies. Recall that the equation of motion derived by Maxey and Riley[19] can only be applied to a particle in a turbulent field if the restrictions on the particle Reynolds number and on the Kolmogorov length scale hold. The preceding analysis shows that the virtual mass contribution for particles with densities differing from the fluid density is relevant only when the displacement amplitude is of the order of or smaller than the particle radius. Because the Kolmogorov length scale of a turbulent flow must be much larger than the radius of the particle to make the formulation valid, virtual mass effects in Eulerian–Lagrangian modeling of particle dispersion in turbulent flows cannot be modeled with this approach for any fluid-to-particle density ratio much different than 1.

In fact, taking the Kolmogorov timescale τ_K as Ω^{-1} implies a Kolmogorov length scale $\eta_K^2 = \nu\tau_K = \nu/\Omega$, which indicates that, to satisfy $\eta_K \gg a$, the dimensional forcing frequency has to be much smaller than $\Omega_{S=1} = 9\nu/a^2$. This restriction implies that only the particulate flows that are in the steady-state Stokes regime $\Omega \ll \Omega_{S=1}$ satisfy the Kolmogorov length scale restriction. Thus, when the Maxey–Riley[19] equation can be employed to model turbulence interactions with a particle, virtual mass effects are necessarily unimportant. Because of the intermediate (half) scale of the history term, the unsteady drag contribution can be important if the Kolmogorov length scale is not many orders of magnitude larger than the radius of the particle. This analytical argument gives weight to the numerical results for heavy particles in homogeneous turbulence presented by Mei et al.[10] Note that if the particle Reynolds number is not much smaller than one, the kernel of the history term has a much faster decay rate.[31] However, one should not conclude that the smaller effects of the history term or the Faxén corrections in higher Reynolds number flows are negligible for the determination of particle trajectories.[19,32]

Note that there is an inherent incompatibility in using a stationary analysis to study the forces acting on a particle at small but finite Reynolds number Re_p. This incompatibility arises because of long-term effects of the velocity disturbance on the far stream flowfield. The stationary analysis assumes that the particles and the flow are oscillating indefinitely in time, and therefore, the background flow cannot be assumed to be unperturbed by the particle motion. In other words, if there is enough time for vorticity to be diffused from the surface of the particle to the Oseen[8] distance (see Ref. 31) then convective effects may modify the far-stream condition. This incompatibility was evident in the work of Reeks and McKee,[33] where it was shown that the Lagrangian particle–fluid velocity correlations previously derived by Tchen,[1] Chao,[28] and Hinze[25] incurred an error. Reeks and McKee's[32] analysis showed that, if the classical kernel of the history term is considered valid for long times, the initial condition would strongly affect the long-term diffusion coefficient of the particle. Mei and Adrian[34] pointed out that the history term decay for long times at small but finite Reynolds number Re_p has to be much faster than the classical $t^{-1/2}$ result obtained for infinitesimal Reynolds number Re_p, thus explaining the apparent paradox. As mentioned before, the faster decay for long times and finite Reynolds number Re_p has been confirmed by other investigations.[5,31]

Given the preceding discussion, it is clear that the relevance of the stationary analysis for real flows is limited. On one hand, the stationary analysis neglects the initial transients and, therefore, cannot be applied in the short-term limit. On the other hand, the main premise of the stationary analysis is in conflict with the long-term effects of the particle motion at finite Reynolds number Re_p, and, therefore, the long-term predictions of the stationary analysis may not represent a good model for particle motion. In general, the classical history kernel given by Eq. (1) should not be used for long-term predictions. However, at infinitesimal Reynolds number Re_p, the classical kernel is relevant and accurate for short times. The present work shows that an analytical treatment of the initial transients is possible. All results shown in Figs. 4–9 refer to the short-time behavior where not enough time has elapsed for vorticity to propagate to the Oseen[8] distance.

VII. Conclusions

A fractional-calculus scaling analysis of the forces that depend on the fluid–particle relative velocity in harmonic Stokes flows past a spherical particle yielded the value of a critical forcing frequency

for which history term effects are maximum. The scaling analysis is validated against the exact analytical solution of the particle equation of motion for a harmonic background flows. Depending on the forcing frequency, the forces acting on the particle can be dominated by either the steady-state Stokes drag (low frequencies) or by virtual mass effects (at high frequencies). When the forcing frequency is of the order of the critical frequency $9\nu/a^2$, all forces are of same order of magnitude and must be considered. The scaling analysis also showed that the displacement of the fluid oscillations must be of the order of the particle radius or smaller to satisfy the small particle Reynolds number restriction.

The critical frequency for maximum history effects depends directly on the kinematic viscosity of the fluid and inversely on the square of the radius of the particle. The analysis also showed that the required restriction of $\eta_K \gg a$ for using Eq. (1) to calculate particle motion in turbulent flows confines the use of this equation to values of forcing frequencies much smaller than the critical value of $9\nu/a^2$. Depending on the ratio η_K/a, history effects can still account for a fraction of the total drag. In other words, Eulerian–Lagrangian formulations of particle motion in turbulent flows for which $\eta_K \gg a$ need not include virtual mass effects, even for bubbly flows. The history force effect can still be felt for flows with a Kolmogorov length scale that is not many orders of magnitude larger than the particle radius because history effects decay slowly for flows departing from the critical frequency range. When the Kolmogorov length scale is many orders of magnitude larger than the radius of the particle, history effects are also negligible. By the use of a different scaling argument, Maxey and Riley[19] indicated that the importance of the history drag and the virtual mass term was indeed limited by the Kolmogorov length scale restriction. The presented analysis shows that a forcing frequency of the order of the critical value of $9\nu/a^2$ is never attained when $\eta_K \gg a$. If the restriction on the Kolmogorov length scale is not satisfied, Eq. (1) or its variations should not be used, and conclusions on the relative importance of forces found by use of this equation have no meaning.

Acknowledgments

This work was supported in part by a grant from NASA Marshall Space Flight Center for the flight definition experiment Spaceflight Holography Investigation in a Virtual Apparatus in collaboration with Metrolaser, Inc. A substantial portion of this research was performed during C.F.M.C Oimbra's stays at the University of California, Irvine, and at Drexel University, Philadelphia.

References

[1]Tchen, C. M., "Mean Value and Correlation Problems Connected with the Motion of Small Particles Suspended in a Turbulent Fluid," Ph.D. Dissertation, Technical School, Delft Univ., Delft, The Netherlands, July 1947.

[2]Trolinger, J. D., Rottenkolber, M., and Elandaloussi, F., "Development and Application of Holographic Particle Image Velocimetry Techniques for Microgravity Applications," *Measurement Science and Technology*, Vol. 8, 1997, pp. 1573–1583.

[3]Stokes, G. G., "On the Theories of Internal Friction of Fluids in Motion," *Transactions of the Cambridge Philosphical Society*, Vol. 8, 1845, pp. 287–305.

[4]White, F. M., *Viscous Fluid Flow*, 2nd ed., McGraw–Hill, New York, 1991, p. 177.

[5]Kim, I., Elghobashi, S., and Sirignano, W. A., "On the Equation for Spherical Particle Motion: Effects of Reynolds and Acceleration Numbers," *Journal of Fluid Mechanics*, Vol. 367, 1998, pp. 221–253.

[6]Boussinesq, J., "Sur la Résistance qu'Oppose un Liquide Indéfini en Repos, sans Pesanteur, au Mouvement varié d'une Sphére Solide qu'il Mouille sur Toute sa Surface, quand les Vitesses Restent Bien Continues et Assez Faibles pour que leurs Carrés et Produits soient Négligeables," *Comptes Rendus Academie des Sciences Paris*, Vol. 100, 1885, pp. 935–937.

[7]Basset, A. B., "On the Motion of a Sphere in a Viscous Liquid," *Philosophical Transactions of the Royal Society of London, Series A: Mathematical and Physical Sciences*, Vol. 179, 1888, pp. 43–63; also *A Treatise on Hydrodynamics*, 1961, Dover, New York, Chap. 22.

[8]Oseen, C. W., *Hydromechanik*, Akademische Verlag, Leipzig, Germany, 1927.

[9]Boggio, T., "Integrazione dell'Equazione Funzionale che Regge la Caduta di una Sfera in un Liquido Viscoso," *Atti dell'Accademia Nazionale dei Lincei, Rendiconti*, Vol. 16, 1907, pp. 730–737.

[10]Mei, R., Adrian, R. J., and Hanratty, J., "Particle Dispersion in Isotropic Turbulence under Stokes Drag and Basset Force with Gravitational Settling," *Journal of Fluid Mechanics*, Vol. 225, 1991, pp. 481–495.

[11]Happel, J., and Brenner, H., *Low Reynolds Number Hydrodynamics*, Prentice–Hall, Englewood Cliffs, NJ, 1975, Chaps. 2, 4, 5.

[12]Lawrence, C. J., and Weinbaum, S., "The Force on an Axisymmetric Body in Linearized, Time-Dependent Motion: A New Memory Term," *Journal of Fluid Mechanics*, Vol. 171, 1986, pp. 209–218.

[13]Lawrence, C. J., and Weinbaum, S., "The Unsteady Force on a Body at Low Reynolds Number; the Axisymmetric Motion of a Spheroid," *Journal of Fluid Mechanics*, Vol. 189, 1988, pp. 463–489.

[14]Feng, J., and Joseph, D.D., "The Unsteady Motion of Solid Bodies in Creeping Flows," *Journal of Fluid Mechanics*, Vol. 303, 1995, pp. 83–102.

[15]Corrsin, S., and Lumley, J., "On the Equation of Motion for a Particle in Turbulent Fluid," *Applied Scientific Research*, Vol. 6A, 1956, pp. 114–116.

[16]Soo, S. L., *Fluid Dynamics of Multiphase Systems*, Blaisdell, Waltham, MA, 1975, pp. 57–67.

[17]Gitterman, M., and Steinberg, V., "Memory Effects in the Motion of a Suspended Particle in a Turbulent Fluid," *Physics of Fluids*, Vol. 23, No. 11, 1980, pp. 2154–2167.

[18]Auton, T. R., Hunt, J. C. R., and Proud'Homme, M., "The Force Exerted on a Body in Inviscid Unsteady Non-Uniform Rotational Flow," *Journal of Fluid Mechanics*, Vol. 183, 1988, pp. 199–218.

[19]Maxey, M. R., and Riley, J. J., "Equation of Motion for a Small Rigid Sphere in a Nonuniform Flow," *Physics of Fluids*, Vol. 26, No. 4, 1983, pp. 883–888.

[20]Coimbra, C. F. M., and Rangel, R. H., "General Solution of the Particle Momentum Equation in Unsteady Stokes Flows," *Journal of Fluid Mechanics*, Vol. 370, 1998, pp. 53–72.

[21]Sy, F., Taunton, J. W., and Lightfoot, E. N., "Transient Creeping Flow Around Spheres," *AIChE Journal*, Vol. 16, No. 3, 1970, pp. 386–391.

[22]Konopliv, N., "Gravitationally Induced Acceleration of Spheres in Creeping Flow—a Heat Transfer Analogy," *AIChE Journal*, Vol. 17, No. 6, 1971, pp. 1502, 1503.

[23]Michaelides, E. E., "A Novel Way of Computing the Basset Term in Unsteady Multiphase Flow Computations," *Physics of Fluids A*, Vol. 4, No. 7, 1992, pp. 1579–1582.

[24]Landau, L. D., and Lifshitz, E. M., *Fluid Mechanics*, 2nd ed., Pergamon, New York, 1978, pp. 83–92.

[25]Hinze, O., *Turbulence*, 2nd ed., McGraw–Hill, New York, 1975, pp. 460–471.

[26]Hjelmfelt, A. T., and Mockros, L. F., "Motion of Discrete Particles in Turbulent Fluid," *Applied Scientific Research*, Vol. 16, 1966, pp. 148–161.

[27]Morrison, F. A., and Stewart, M. B., "Small Bubble Motion in an Accelerating Fluid," *Journal of Applied Mechanics*, Vol. 97, Sept. 1976, pp. 399–402.

[28]Chao, B. T., "Turbulent Transport Behavior of Small Particles in Dilute Suspension," *Ósterreichisches Ingenieur-Archiv*, Vol. 18, Aug.–Nov. 1968, pp. 7–21.

[29]Friedlander, S. K., "Behavior of Suspended Particles in a Turbulent Fluid," *AIChE Journal*, Vol. 3, No. 3, 1957, pp. 381–388.

[30]Oldham, K. B., and Spanier, J., *The Fractional Calculus*, Academic Press, New York, 1974, pp. 80, 81.

[31]Lovalenti, P. M., and Brady, J. F., "The Hydrodynamic Force on a Rigid Particle Undergoing Arbitrary Time-Dependent Motion at Small Reynolds Number," *Journal of Fluid Mechanics*, Vol. 256, 1993, pp. 342–356.

[32]Peng, F., and Aggarwal, S. K., "Effects of Flow Nonuniformity and Relative Acceleration on Droplet Dynamics," *Atomization and Sprays*, Vol. 6, No. 1, 1996, pp. 51–76.

[33]Reeks, M. W., and McKee, S., "The Dispersive Effects of Basset History Forces on Particle Motion in a Turbulent Flow," *Physics of Fluids*, Vol. 27, No. 7, 1984, pp. 1573–1582.

[34]Mei, R. W., and Adrian, R. J., "Flow Past a Sphere with an Oscillation in the Free-Stream Velocity and Unsteady Drag at Finite Reynolds Number," *Journal of Fluid Mechanics*, Vol. 237, 1992, pp. 323–341.

S. K. Aggarwal
Associate Editor